Histol Histopathol (2023) 38: 29-46

**http://www.hh.um.es**

Histology and Histopathology
*From Cell Biology to Tissue Engineering*

**ORIGINAL ARTICLE** **Open Access**

# Intussusceptive angiogenesis facilitated by microthrombosis has an important example in angiolipoma. An ultrastructural and immunohistochemical study

**Lucio Díaz-Flores[1], Ricardo Gutiérrez[1], Maria Pino García[2], Miriam González-Gómez[1,3], Lucio Díaz-Flores Jr[1], Jose Luis Carrasco[1], Juan Francisco Madrid[4] and Hugo Álvarez-Argüelles[1]**

[1]Department of Basic Medical Sciences, Faculty of Medicine, University of La Laguna, [2]Department of Pathology, Eurofins Megalab-Hospiten Hospitals, [3]Instituto de Tecnologías Biomédicas de Canarias, University of La Laguna, Tenerife and [4]Department of Cell Biology and Histology, School of Medicine, Campus of International Excellence "Campus Mare Nostrum", IMIB-Arrixaca, University of Murcia, Murcia, Spain

**Summary.** The microvasculature of angiolipoma frequently presents thrombi. Our objectives are to assess whether intussusceptive angiogenesis (IA) participates in vasculature formation in non-infiltrating angiolipoma and, if so, to explore how thrombi are involved in the IA process. For this purpose, we studied angiolipoma specimens (n: 52), using immunohistochemistry, and confocal and electron microscopy. The results showed the presence of folds and pillars, hallmarks of IA, dividing the vessel lumen. Folds showed a cover formed by reoriented endothelial cells from the vessel wall, or from newly formed folds, and a core initially formed by thrombus fragments (clot components as transitional core), which was replaced by extracellular matrix and invaginating pericytes establishing numerous peg-and-socket junctions with endothelial cells (mature core). A condensed plasmatic electron-dense material surrounded and connected folds and pillars with each other and with the vascular wall, which suggests a clot role in fold/pillar arrangement. In conclusion, we contribute to IA participation in capillary network formation in angiolipoma and the immunohistochemical and ultrastructural events by which microthrombosis facilitates IA. Therefore, in addition to the histogenesis of angiolipoma, we provide an easily obtainable substrate for future studies on clot component action in IA, of clinical and therapeutic interest.

*Corresponding Author:* Lucio Díaz-Flores, Department of Basic Medical Sciences, Faculty of Medicine, University of La Laguna, 38071 Tenerife, Spain. e-mail: kayto54@gmail.com

DOI: 10.14670/HH-18-488

**Key words:** Angiogenesis, Intussusceptive angiogenesis, Angiolipoma, Microcirculation, Thrombi, Coagulation, Pericytes, Endothelial cells

## Introduction

Sprouting and intussusceptive angiogenesis are the two principal types of angiogenesis in physiological and pathological conditions (Folkman, 1971; Burri and Tarek, 1990). These angiogenic types can have complementary mechanisms, with synergistic interaction (Karthik et al., 2018; Díaz-Flores et al., 2020a). In sprouting angiogenesis, vessel sprouts grow out of a microvasculature by overlapping sequential mechanisms, which include migration of endothelial cells (ECs), changes in extracellular matrix with basement membrane degradation, proliferation of ECs, mobilization, proliferation and recruitment of pericytes and perivascular CD34+ stromal cells/telocytes, participation of inflammatory cells, tubulogenesis (vascular lumen development), formation of a new basement membrane and vessel fusion, pruning, and stabilization (Ribatti and Crivellato, 2012; Díaz-Flores et al., 2017a; Eelen et al., 2020). Microvascular growth, vessel arborization, branching remodeling, and vessel segmentation from a pre-existing microvasculature can occur in intussusceptive angiogenesis (IA) (Patan et al., 2001a,b; Burri and Djonov, 2002; Djonov et al., 2002, 2003; Burri et al., 2004; Makanya et al., 2009; De Spiegelaere et al., 2012; Ackermann et al., 2013; Mentzer and Konerding, 2014; Díaz-Flores et al., 2018a). The main mechanism in IA is the formation of intravascular tissue folds and pillars (columns or posts),

which partially or totally divide the vessel lumen and increase or remodel the vascular network (Caduff et al., 1986; Burri, 1990, 1992; Burri and Tarek, 1990; Patan et al., 1996a; Djonov et al., 2000a,b; Augustin, 2001; Burri et al., 2004; Paku et al., 2011). Thrombosis can be observed in association with IA, as occurs in Covid-19 disease (Ackermann et al., 2020) and in intravascular papillary endothelial hyperplasia (Díaz-Flores et al., 2021a). An immunohistochemical and ultrastructural study of an easily obtainable entity in which thrombosis in small vessels (microthrombosis) and IA were associated mechanisms is of interest to assess the events during coagulation and intraluminal tissue fold and pillar formation.

Non-infiltrating angiolipoma is a circumscribed lesion composed by mature adipose tissue and clusters of small, branched capillaries, predominantly located in the periphery (Lin and Lin, 1974; Charifa et al., 2021). Hyaline/fibrin microthrombi are almost always observed in the capillaries of angiolipoma (Charifa et al., 2021), and IA has not been explored in this process. An immunohistochemical and ultrastructural study is appropriate to assess whether IA occurs in vessels of angiolipoma and whether microthrombosis participates in tissue fold and pillar formation. If so, this study is not only of interest to explain angiolipoma histogenesis, but also to know the events that occur in the association of thrombosis/IA, which can be a basis for future research on the role of coagulation in IA, of clinical and therapeutic interest. This interest is greater due to the complementarity between IA and sprouting angiogenesis, which IA can follow (Díaz-Flores et al., 2017a, 2020a; Karthik et al., 2018). Thus, in several processes, including tumors, vessel splitting with microvascular growth can occur by IA mechanisms after the formation of neo-vessels by sprouting angiogenesis, requiring subsequent studies on changes in anti-angiogenesis treatment, in which possible modulators of IA have not sufficiently performed (Eelen et al., 2020).

Given the above, the first objective of our study is to assess whether IA participates in capillary network formation in angiolipoma. This being the case, the second objective is to explore whether the thrombi are involved in the formation, arrangement, and connections of the intussusceptive tissue folds and pillars, and what immunohistochemical and ultrastructural events occur during their participation in these mechanisms.

## Materials and methods

### *Human tissue samples*

The archives of Histology and Anatomical Pathology of the Departments of Basic Medical Sciences of La Laguna University, University Hospital, and Eurofins® Megalab-Hospiten Hospitals of the Canary Islands were searched for cases of angiolipoma. Paraffin blocks were obtained from surgical specimens of 52 Caucasian patients. The samples of the 52 cases were studied by conventional histologic techniques. From them, cases with more abundant vessels and presence of microthrombi (n: 32) were used for immunochemistry procedures and immunofluorescence in confocal microscopy. Two cases were obtained for electron microscopy observation. Ethical approval for this study was obtained from the Ethics Committee of La Laguna University (Comité de Ética de la Investigación y de Bienestar Animal, CEIBA2022-3124), including the dissociation of the samples from any information that could identify the patient. The authors therefore had no access to identifiable patient information.

### *Light microscopy*

Specimens for conventional light microscopy were fixed in a buffered neutral 4% formaldehyde solution, embedded in paraffin, and cut into 3 μm-thick sections. Sections were stained with Haematoxylin and eosin, Trichrome staining (Roche, Basel, Switzerland. Ref. 6521908001), and Reticulin staining (Roche, Ref. 05279399001).

### *Immunohistochemistry*

Histologic sections, 3 μm-thick, were attached to silanized slides. After pre-treatment for enhancement of labeling, the sections were blocked with 3% hydrogen peroxide and then incubated with primary antibodies (10–40 minutes). The primary antibodies used in this study were CD34 monoclonal mouse anti-human, clone QBEnd-10, (dilution 1:50), catalog No. IR632 (Dako, Glostrup, Denmark), α-smooth muscle actin (αSMA) monoclonal mouse anti-human, clone 1A4 (dilution 1:50), catalog No. IR611 (Dako, Glostrup, Denmark), rabbit polyclonal anti-vascular endothelial growth factor A (VEGF-A), (dilution 1:200), catalog No. sc-507 (Santa Cruz Biotechnology, Heidelberg, Germany) and rabbit polyclonal anti-TNFα, (dilution 1:500), catalog No. ab66579 (Abcam, Cambridge, UK).The immunoreaction was developed in a solution of diaminobenzidine, and the sections were then briefly counterstained with hematoxylin, dehydrated in ethanol series, cleared in xylene, and mounted in Eukitt®. Positive and negative controls were used. For the double immunostaining, we used anti-CD34 antibody (diaminobenzidine, DAB, as chromogen) to highlight CD34+ ECs and anti-αSMA (aminoethylcarbazole, AEC, substrate-chromogen) for anti-αSMA+ pericytes/smooth muscle cells.

### *Immunofluorescence in confocal microscopy*

For immunofluorescence, tissue sections of 6 and 10 μm were obtained. For antigen retrieval, sections were deparaffinized and boiled for 20 minutes in sodium citrate buffer 10 mM (pH 6), rinsed in Tris-buffered saline (TBS, pH 7.6, 0.05 M), and incubated with the following primary antibodies diluted in TBS overnight in a humid chamber at room temperature: mouse

monoclonal anti-CD34, code no. IR63261 (ready to use) and rabbit polyclonal anti-collagen IV (1/500 dilution, code no. ab6586, Abcam). For the double immunofluorescence staining, sections were incubated with a mixture of monoclonal and polyclonal primary antibodies (mouse monoclonal anti-CD34 and rabbit polyclonal anti-collagen IV). The next day, the slides were rinsed in TBS and incubated for 1 hour at room temperature in the dark with the secondary biotinylated goat anti-rabbit IgG (H+L) (1:500, Code: 65-6140, Invitrogen, San Diego, CA, USA) and Alexa Fluor 488 goat antimouse IgG (H+L) antibody (1:500, Code: A11001, Invitrogen), followed by incubation with Streptavidin Cy3 conjugate (1:500, Code: SA1010, Invitrogen) for 1 hour at room temperature in the dark. Nuclei were detected by DAPI staining (Chemicon International, Temecula, CA, USA). After washing in TBS, sections were exposed to a saturated solution of Sudan black B (Merck, Barcelona, Spain) for 20 minutes to block autofluorescence. They were rinsed in TBS and cover-slipped with DABCO (1%) and glycerol-PBS (1:1). Negative controls were performed in the absence of primary antibodies. Fluorescence immunosignals were obtained in a Fluoview 1000 laser scanning confocal imaging system (Olympus Optical), using the objective 60×/1.35 oil.

### *Electron microscopy*

Specimens for electron microscopy (ultrathin sections) were initially fixed in glutaraldehyde solution, diluted to 2% with sodium cacodylate buffer, pH 7.4, for 6 hours, at 4°C. They were then washed in the same buffer, post-fixed for 2 hours in 1% osmium tetroxide, dehydrated in a graded ethanol series, and embedded in epoxy resin. Ultrathin sections were double stained with uranyl acetate and lead citrate. The grids were examined with a JEOL® 100B and JEM 1011 Akishima, Tokyo, Japan, electron microscopes.

## Results

### *General characteristics of angiolipomas*

Angiolipomas were well-circumscribed and showed clusters of small vessels, predominantly capillaries, intermixed with mature adipose tissue (Fig. 1A). The density of vascularization varied depending on the case, and the vessel clusters were more numerous in the periphery of the lesion. The vessels ranged from round or oval to irregular, tortuous, and branched. Aggregates of red blood cells and hyaline/fibrin microthrombi were observed in a varying number of vessels, many of them dilated (Fig. 1A–C). The microthrombi were formed by strands of fibrin filaments (Fig. 1D) and platelets. Some microthrombi appeared fragmented (hereinafter, microthrombus or its fragments: thrombus). ECs were ultrastructurally observed around several thrombi (Fig. 1E), some of which contained numerous platelets (Fig. 1E).

### *Thrombus endothelialization by vessel wall ECs and formation of intravascular (intraluminal) tissue folds*

The vessel wall ECs appeared reoriented from the vessel wall and continued with those around the thrombus, leaving a thrombotic region, which converged with the interstitium (Fig. 2A,B). In these thrombi surrounded by ECs, newly formed extracellular matrix and pericytes or pericyte processes were observed in continuity with the convergent thrombus/interstitium region (passage of pericytes to the thrombus) (Fig. 2A,B). Pericytes extending between both sides in which the ECs curve and reorient to cover the thrombus were frequently observed (Figs. 2A, 3, 4A).

The covering ECs, the thrombus components, the newly formed extracellular matrix and their incorporated pericytes appeared as an intraluminal tissue fold in the vascular lumen (Fig. 2A,B). Therefore, each intraluminal tissue fold showed a cover made up of the lining ECs and a core formed by residual thrombotic components, penetrating pericytes, and extracellular matrix (Fig. 2A,B). The pericytes that invaded the thrombus and contributed to form the intraluminal tissue fold showed an electron rare cytoplasm (Fig. 2A) and SMA expression by double immunochemistry for CD34 and αSMA (Fig. 2B). A thick layer formed by extracellular membranous material was observed between ECs and pericytes (Fig. 2A). CD34+ perivascular stromal cells/telocytes were present around the vessels (Fig. 3) and occasionally invading the thrombus. The folds did (Fig. 3A,B) or did not (Fig. 2A,B) reach the opposite side of the vessel. When they did, they were observed in cross sections as a large pillar separating two new vessels (Fig. 3A,B).

Association between pericytes and ECs was observed in the folds, with frequent establishment of heterocellular peg-and-socket junctions, in which pericytes originated the peg and ECs formed the socket in their abluminal surface (Figs. 2A, 3A, 4C–D) (Figures 4C–D correspond to peg-and-socket junctions between pericytes and ECs at higher magnification from those shown in Figures 2A, 3A). With relative frequency, a pericyte contacted both sides of the fold, forming peg-and-socket junctions with the ECs, above all at the ends of the fold, where the ECs bend to line it (Figs. 4A–C). Association of platelets and ECs was also observed, suggesting that some of the contacting structures were peg-and-socket junctions, like those established between pericytes and ECs (the platelet forms the peg, and the EC forms the socket) (Fig. 2A).

The newly formed extracellular matrix corresponded predominantly to collagen IV (see below). Occasionally, collagen I was observed.

Secondary folds were seen forming on primary folds (segmentation of folds) (Fig. 5A,B), reaching other regions of the vessel wall by means of these new folds (Fig. 5B) or pillars (see below). Lining ECs of a fold

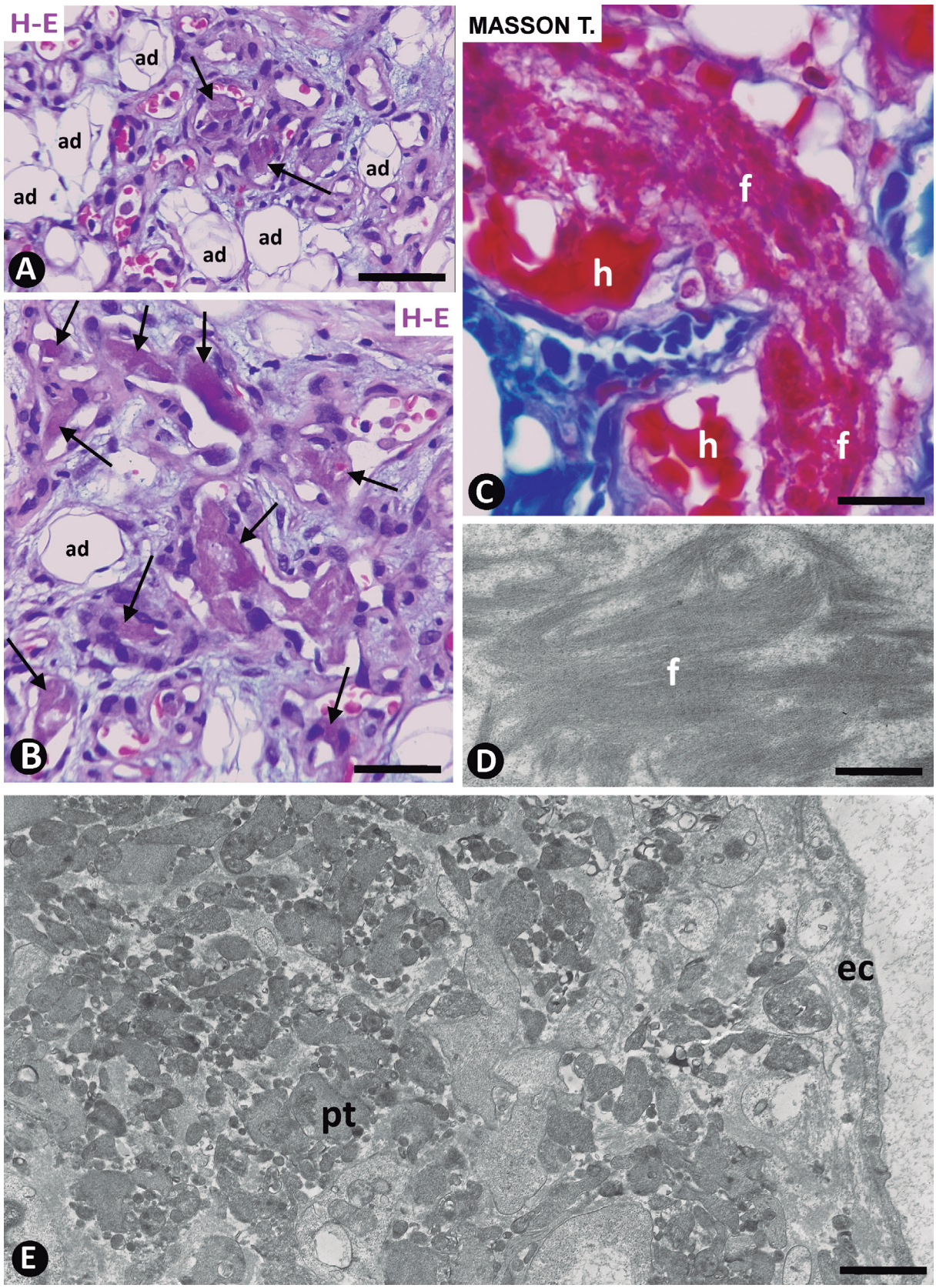


**Fig. 1.** General characteristics of angiolipoma. **A, B.** Clusters of small vessels are observed between adipocytes (ad) in Hematoxylin and eosin-stained sections. Hyaline/fibrin thrombi are present in the lumen of some vessels (arrows). **C.** Aggregates of red blood cells (h) and fragmented fibrin deposits are seen using Masson's trichrome staining. **D.** Fibrils of the fibrin deposits (f) observed under electron microscopy. **E.** Ultrastructural image showing thrombotic components, including modified platelets (pt) and cell debris, surrounded by thin extensions of endothelial cells (ec). A,B: Hematoxylin–eosin staining. C: Masson's staining. D,E: Ultrathin sections. Uranyl acetate and lead citrate. Scale bars: A, 120 $\mu$m; B, 60 $\mu$m; C, 25 $\mu$m; D, 2.5 $\mu$m, E, 4 $\mu$m.

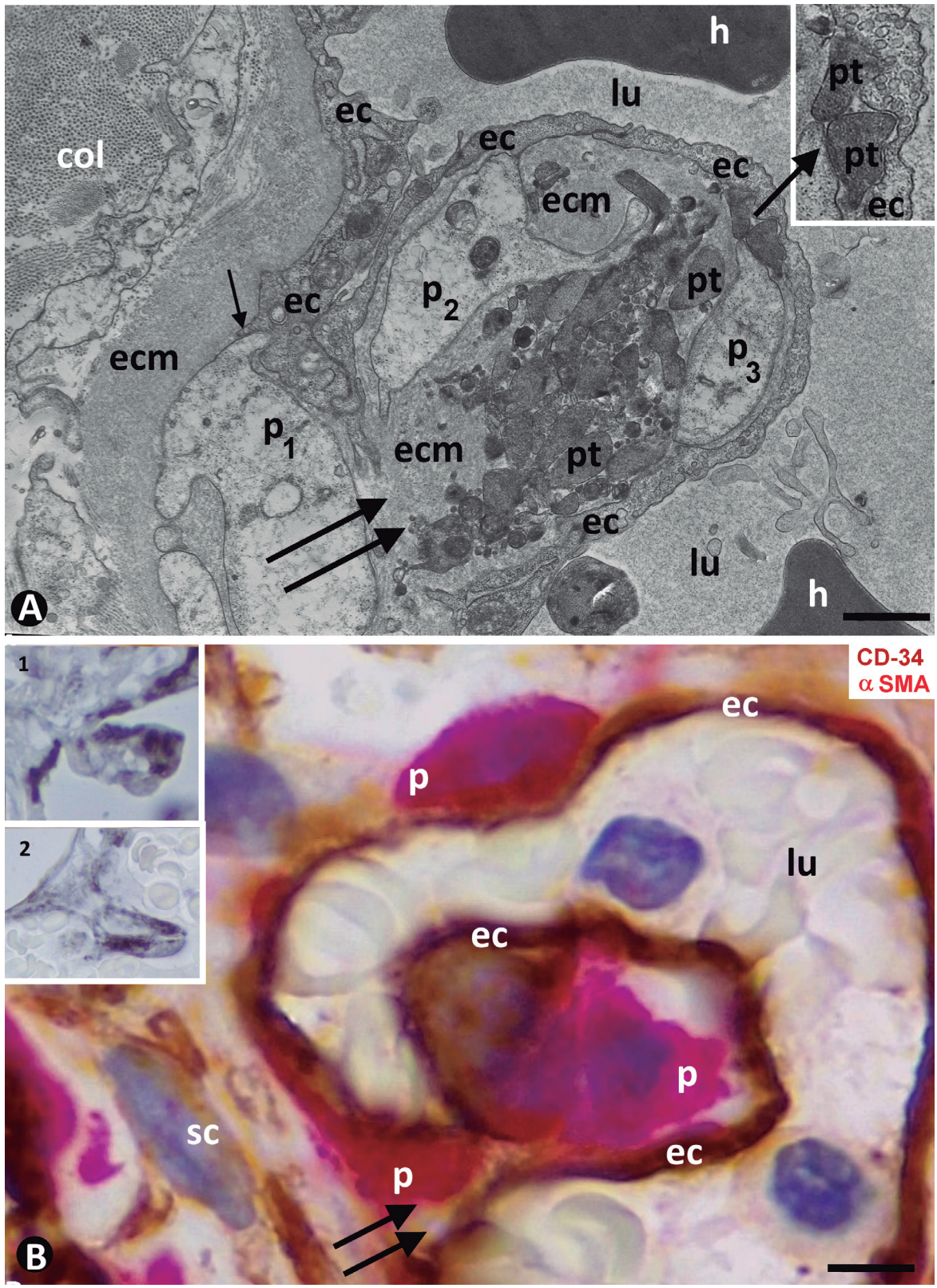


**Fig. 2.** Presence of folds in the vessel lumen of angiolipomas. **A.** Ultrastructural image of a fold with ECs (ec) surrounding residual thrombotic components, pericytes (p1–p3) and extracellular matrix (ecm). Note that the vessel ECs extend and form the fold cover (reoriented vessel ECs) and that the surrounded components form the core. A pericyte (p1) forms a peg-and-socket junction with an EC (arrow) (see Fig. 4C at higher magnification). Insert: Two platelets (pt), at higher magnification, associated with an EC suggesting formation of peg-and-socket junctions. **B.** CD34+ ECs (brown) and αSMA+ pericytes (red) are observed in a fold cover and core, respectively. Note in A and B a region in which the core of the fold contacts with the interstitium (double arrows). In inserts 1 and 2, expression of VEGF-A and TNFα in tissue folds are respectively observed. EC: ec. Pericytes: p. platelet: pt. Extracellular matrix: ecm. Collagen: col. Vessel lumen: lu. Red blood cells: h. CD34+ perivascular stromal cell/telocyte: sc. A: Ultrathin section. Uranyl acetate and lead citrate. B: Double immunochemistry for CD34 (brown) and SMA (red). Scale bars: A, 4 $\mu$m; B, 10 $\mu$m.

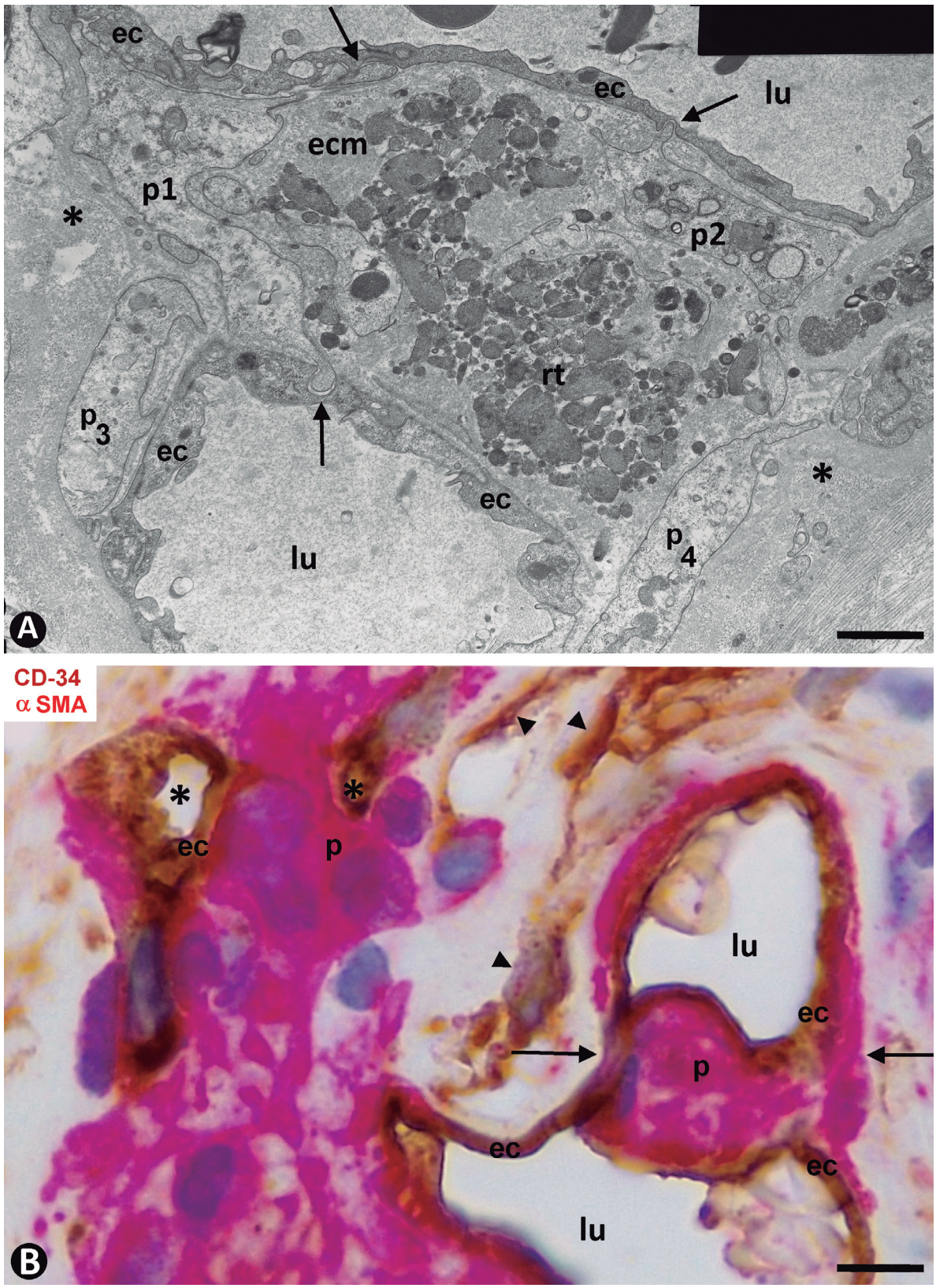


**Fig. 3.** Ultrastructural **(A)** and immunochemical **(B)** observation of longitudinally sectioned folds, which extend between the opposite sides of the vessels, connect at their ends with the periendothelial region and interstitium (asterisks), and separate into two new vessels. **A.** Pericytes (p1–p4), residual thrombotic components (rt) and extracellular matrix (ecm) in the fold. Note that the pericytes establish peg-and-socket junctions with the ECs (arrows) (see Fig. 4A,B,C at higher magnification). **B.** Immunohistochemical observation of ECs (brown) and pericytes (red) in the fold extending between the opposite sides of a vessel (arrows). Numerous pericytes increased in size (red) and some CD34+ stromal cells/telocytes (arrowheads) are also observed around small vessels (asterisks). EC: ec. Pericyte: p. Vessel lumen: lu. A: Ultrathin section. Uranyl acetate and lead citrate. B: Double immunochemistry for CD34 (brown) and αSMA (red). Scale bars: A, 4 $\mu$m; B, 10 $\mu$m.

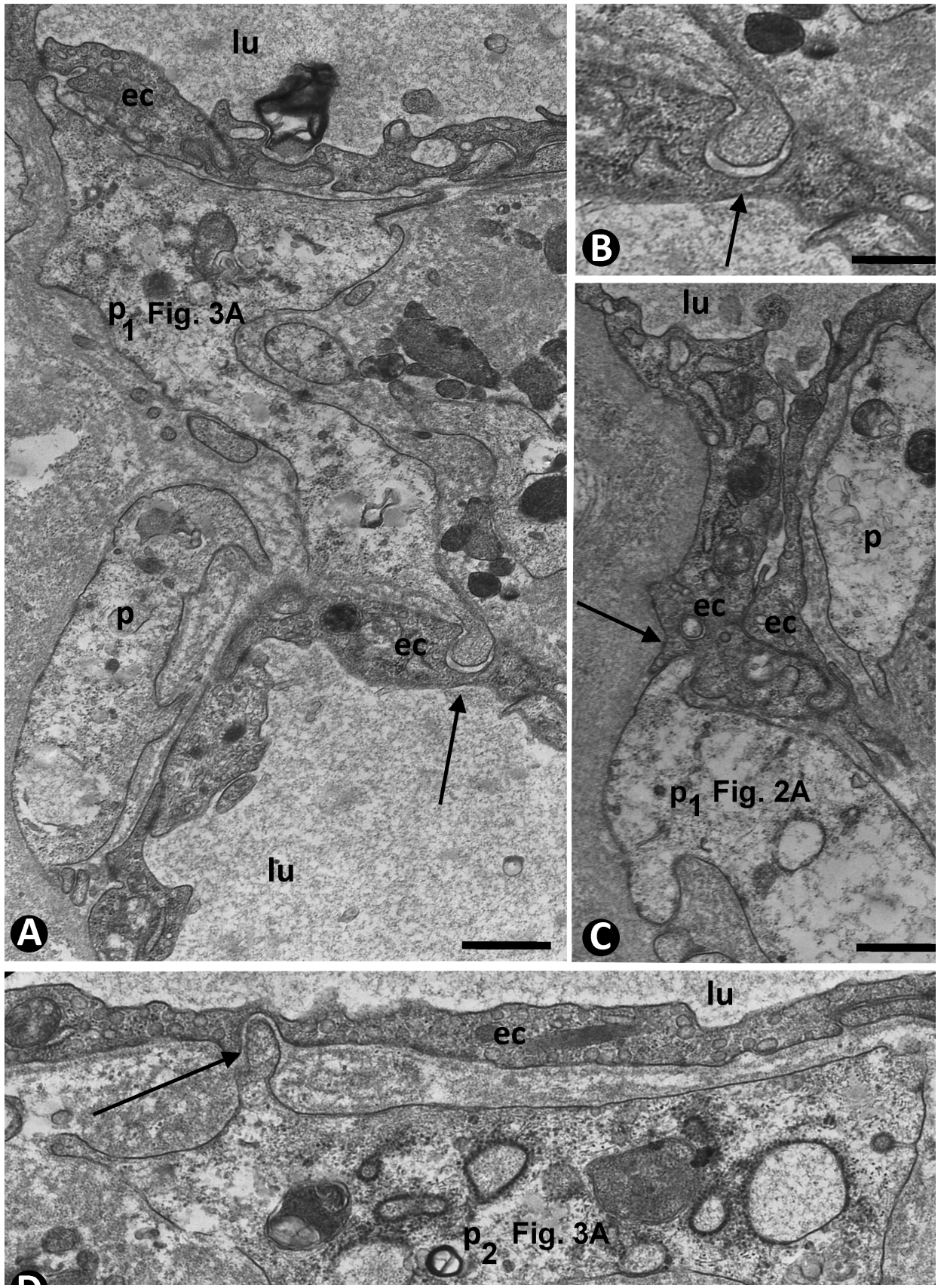


**Fig. 4.** Peg-and-socket junctions established between pericytes and ECs of Fig. 2A and 3A showed a higher magnification (arrows). In these structures, pericytes form the peg and ECs form the socket. Note peg-and-socket joints at the ends of the fold, where the ECs bend and reorient to line the fold **(A–C)**. Endothelial cell: ec. Pericyte: p. Vessel lumen: lu. **A, B.** From p1 of Fig. 3A. **C.** From p1 of Fig. 2A. **D.** From p2 Fig. 3A. **B.** Detail of A. Ultrathin sections. Uranyl acetate and lead citrate. Scale bars: A, C, D, 2 $\mu$m; B, 1.5 $\mu$m.

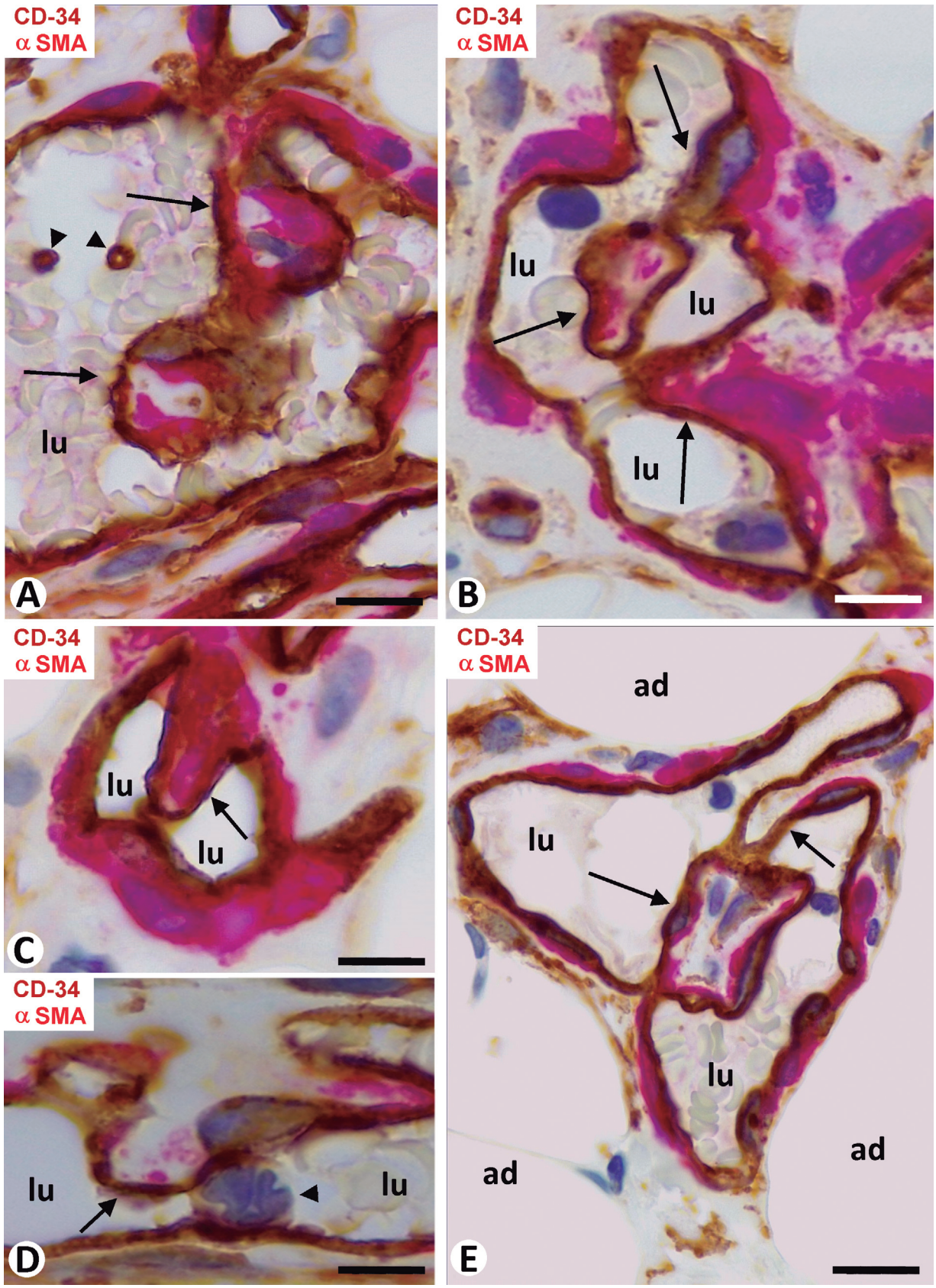


**Fig. 5.** Segmentation and contacts of folds. **A, B.** Segmented folds (arrows), aligned and forming septa that extend toward other points of the vessel wall **(A)** and reach other folds **(B)**. Note in A two cross-sectioned small pillars (arrowheads). **C, D.** Folds (arrows) contacting the opposite vessel wall **(C)** and leaving a narrow space in which a leukocyte (arrowhead) is retained **(D)**. **E.** Convergent folds (arrows) originating from opposite regions of the vessel wall. Cover CD34+ ECs (brown) and core αSMA+ pericytes (red) are observed in folds and pillars. Vessel lumen: lu. Adipocytes: ad. Double immunochemistry for CD34 (brown) and αSMA (red). Scale bars: 15 $\mu$m.

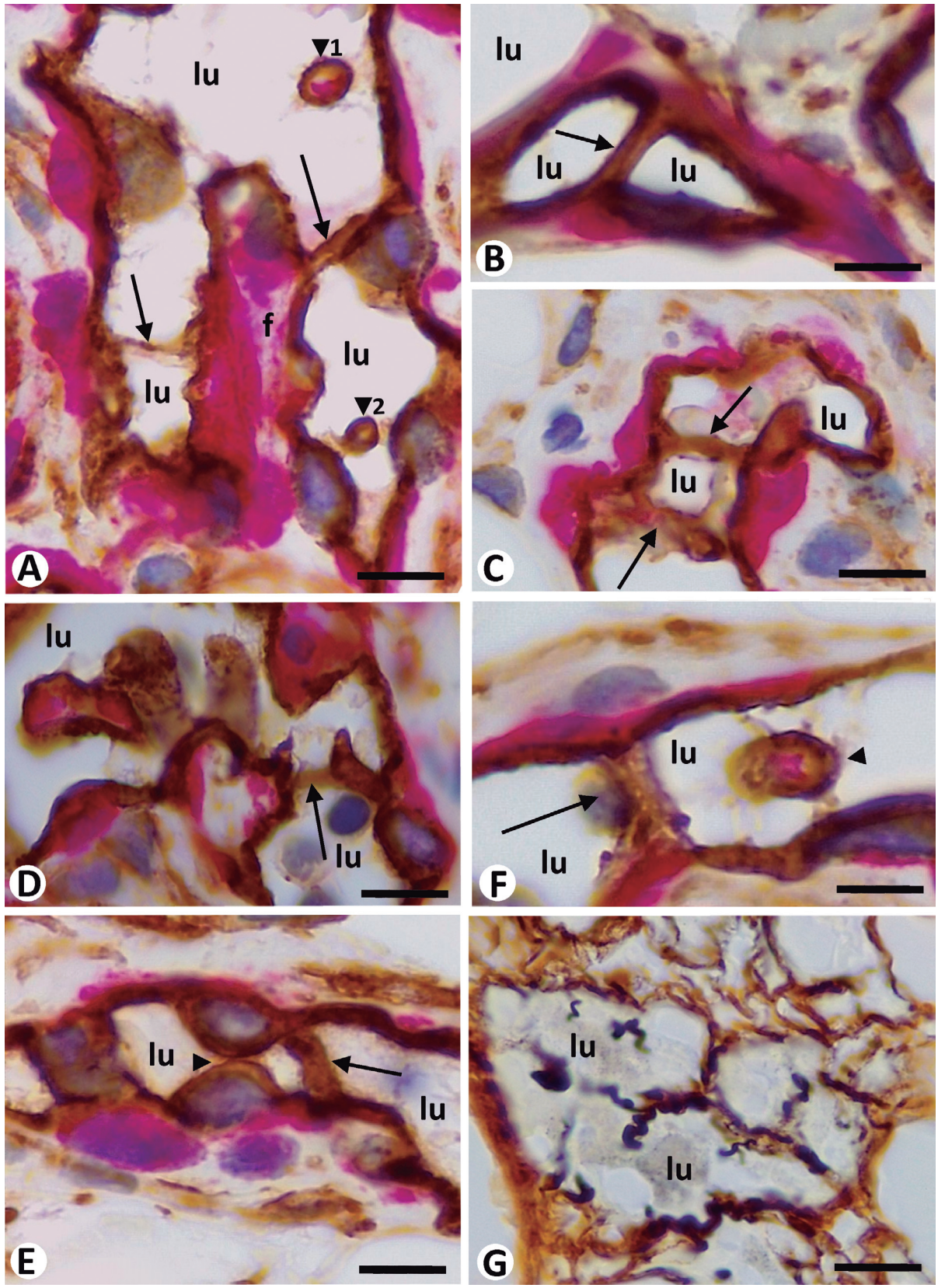


**Fig. 6.** Intravascular pillars. **A.** Longitudinally (arrows) and cross-sectioned (arrowheads) pillars are observed in the lumen of a vessel. Note that the longitudinally sectioned pillars extend between a fold (f) and the vessel wall. The core of a cross-sectioned pillar (arrowhead 1) shows a thin process of a pericyte (red). **B, C.** Pillars (arrows) that extend from one side of the vessel wall to the other side. **D.** Pillars (arrows) between folds. **E.** A pillar (arrow) in proximity to prominent contacting ECs (arrowhead) from two opposite points of the vessel wall. **F.** Thin process of a pericyte in the core of a pillar (arrowhead). **G.** Extracellular matrix with high affinity for reticulin in the core of pillars. Vessel lumen: lu. A–F: Double immunochemistry for CD34 (brown) and αSMA (red). G: Reticulin staining. Scale bars: A-F, 15 $\mu$m; G, 25 $\mu$m.

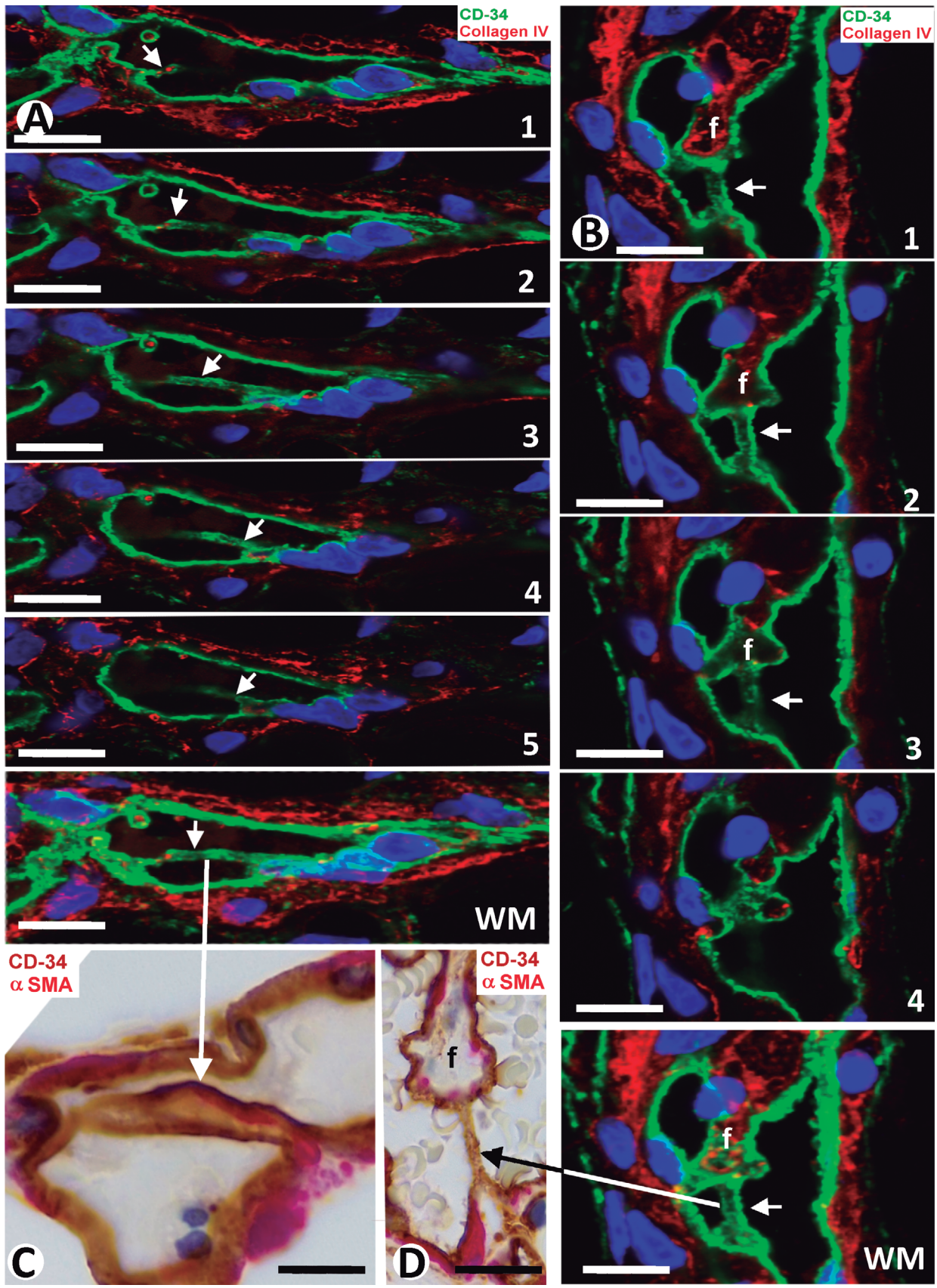


**Fig. 7. A1–5, B1–4.** Appearance and disappearance of pillars (short arrows) in a series of individual visions in confocal microscopy. The pillar in **A1–5** extends from one side of the vessel wall to another. The pillar in **B1–4** extends from a fold to the vessel wall. In A and B, whole mounted visions (WM) are also shown. **C, D.** Similar arrangement of pillars observed by immunochemistry (long arrows). **A,B.** Double immunofluorescence labeling for CD34 and Collagen IV. C, D: Double immunochemistry for CD34 and αSMA. Scale bars: A, B, D, 20 $\mu$m; C, 15 $\mu$m.

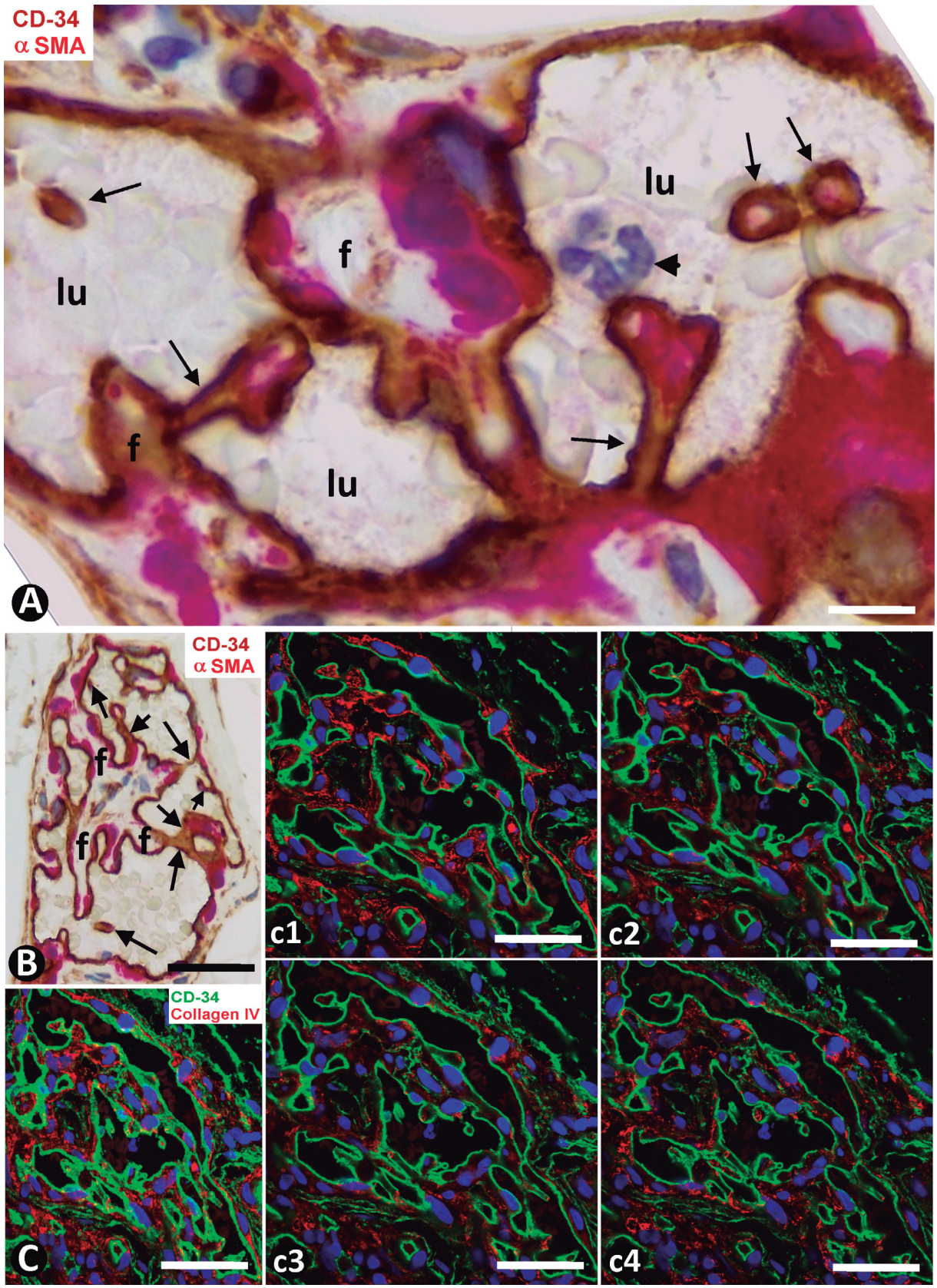


**Fig. 8. A, B.** Associated folds (f) and pillars (arrows) forming complex structures in the lumen of the vessels. Pericyte (red) in the core and ECs (brown) in the cover are present in these structures. Note a leukocyte (arrowhead) between fold/pillars. **C, C1–C4.** Under confocal microscopy, a WM vision **(C)** and series of individual visions **(C1–C4)** show the appearance and disappearance of parts of the complex structures, which present a core with collagen IV (red) and a cover formed by ECs (green). A, B: Double immunochemistry for CD34 and αSMA. C, C1–C4: Double immunofluorescence labeling for CD34 and Collagen IV. Scale bars: A, 10 $\mu$m; B, C, 60 $\mu$m.

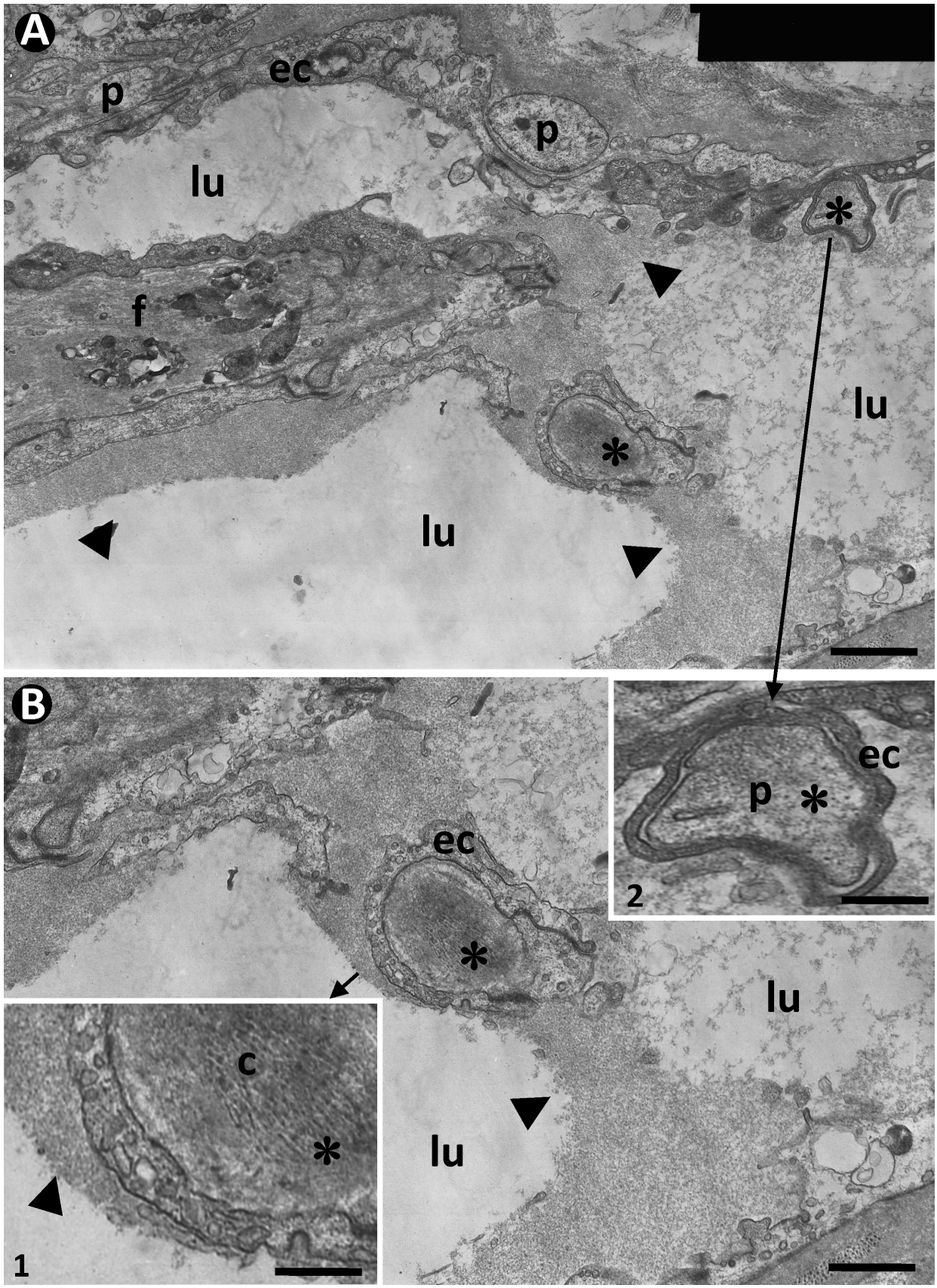


**Fig. 9. A.** Ultrastructural images of a fold (f) and two pillars (asterisks). **B.** Details of the pillars in which collagen (c, insert 1) and a process of a pericyte (p, insert 2 ) are observed in their cores. Note the presence of intraluminal electron-dense material around the fold and a pillar (A,B and insert 1, arrowheads). This electron-dense material binds the fold and the pillar, and the pillar and the vessel wall (A,B, arrowheads). Ultrathin section. Uranyl acetate and lead citrate. Endothelial cell: ec. Vessel lumen: lu. Scale bars: A, 4 $\mu$m; B, 3 $\mu$m; Inserts 1, 2, 0.5 $\mu$m.

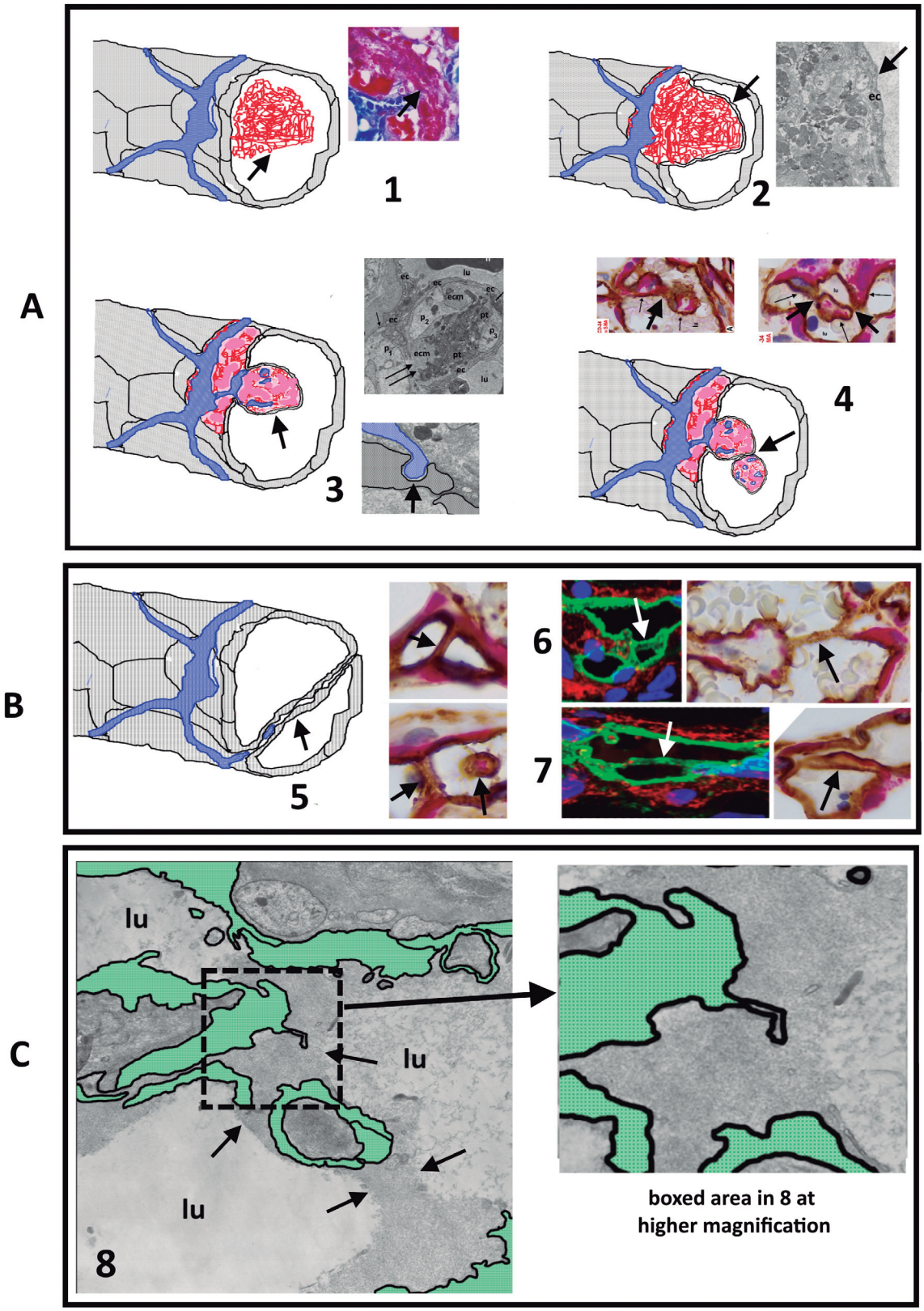


**Fig. 10.** Microthrombosis/IA association and findings (arrows) suggesting the steps in tissue fold and pillar formation. **A.** Steps in tissue fold formation: 1) Microthrombi in capillaries, 2) thrombus delimitation by ECs, 3) regression of most of thrombus components, invasion of pericytes, extracellular matrix formation, establishment of peg and socket junctions between pericytes and ECs, and maturation of tissue folds, 4) establishment of contacts and segmentation of tissue folds, and transluminal fold development. **B.** Steps in pillar formation: 5, 6, 7) intraluminal extensions of ECs with bilayer formation (nascent pillars), incorporation and/or formation of extracellular matrix (collagen IV) and penetration of pericyte processes between the EC bilayer, and association of pillars with intraluminal tissue folds and other pillars, leading to the division of vessel lumens. **C.** Intraluminal condensation of an electron-dense plasmatic material (8), which surround tissue folds and pillars and connect them with the capillary wall.

could simply contact with ECs from other regions of the vessel wall or leave small spaces (Fig. 5C,D). In the latter, red blood cells and leukocytes could be retained (Fig. 5D). Folds originating from opposite regions of the vessel wall could also converge, their lining ECs making contact (Fig. 5E).

*Formation of intravascular pillars (<2.5 μm)*

Vessels presenting intraluminal pillars (<2.5 μm in diameter) were frequently observed in angiolipomas. The pillars in the longitudinal or cross-sectioned vessel lumen (Fig. 6) appeared as endothelial bridges (nascent pillars), EC bilayer, or EC bilayer surrounding a central core. Thus, when cross- sectioned, pillars showed a cover formed by ECs expressing CD34 and a core containing extracellular matrix and thin processes of pericytes in some (Fig. 6A,F). When longitudinally sectioned, the intravascular pillars were seen bridging an intraluminal tissue fold to the vessel wall (Fig. 6A), from one side of the vessel to the other (Fig. 6B,C), or between intraluminal tissue folds (Fig. 6D). Pillars could be near to prominent contacting ECs from two opposite points of the vessel wall (Fig. 6E). Inflections or changes in their orientation were observed in some pillars, which appear incompletely sectioned and occasionally longitudinal and cross-sectioned in the same pillar. The extracellular matrix in the core of the pillars showed high affinity for reticulin (Fig. 6G) and extensive expression for collagen IV (Fig. 7A,B).

Using double immunofluorescence labeling for CD34 and collagen IV in confocal microscopy, in addition to expression for collagen IV in the extracellular matrix, we observed the appearance and disappearance of pillars in a series of individual views (Figs. 7A1–5 and Figs. 7B1–4), a pillar from one point of the vessel wall to another (Fig. 7A1–5), and a pillar from a fold to the vessel wall (Figs. 7B1–4), as well as their images in whole mounted views (Fig. 7A/WM and 7B/WM). These pillars were like those observed by double immunohistochemistry for CD34 and αSMA (Fig. 7C,D).

Associated multiple folds and pillars originating complex structures were seen by immunohistochemistry (Fig. 8A,B) and immunofluorescence (Fig. 8C) in some dilated vessels. Appearance and disappearance of part of these structures were also observed in a series of individual visions in confocal microscopy (Fig. 8C1–4).

In electron microscopy, the pillar cover appeared formed by thin ECs with pinocytotic vesicles (Fig. 9A,B and insert 1 of B), and the pillar core by collagen material (Fig. 9A,B and insert 1 of B). Processes of pericytes in the pillar core (Fig. 9A and insert 2 of B) were also seen under electron microscopy.

The ultrastructural observation revealed an intravascular, fine granular or fibrillar electron-dense material in the lumen of the vessels, surrounding some of the folds and pillars and connecting them to each other and with the vessel wall (Fig. 9A,B and insert 1 of B). The fine electron-dense granules and fibrils of this material appeared loosely arranged and were weakly stained with Masson's Trichrome staining.

## Discussion

In this immunohistochemical and ultrastructural study, we report a) the participation of IA in capillary network development in angiolipoma by formation of intravascular tissue folds and pillars, the hallmarks of IA, and b) the involvement of several mechanisms in this process, in which microthrombosis plays an important role in the intraluminal tissue fold and pillar formation, arrangement, and connection (Fig. 10).

The numerous processes that bridge the vessel lumen in angiolipoma meet the characteristics of intraluminal/transluminal tissue folds (insertion of interstitial tissue structures, diameter >2.5 μm) and pillars (diameter <2.5 μm) (Patan et al., 2001a,b). The components of these structures and the requirements to consider pillars as such have been extensively described (Lin and Lin, 1974; Caduff et al., 1986; Burri and Tarek, 1990; Burri, 1992; Patan et al., 1992, 1993, 1996a,b, 2001a,b; Djonov et al., 2000a,b, 2002, 2003; Burri and Djonov, 2002; Kurz et al., 2003; Burri et al., 2004; Patan, 2008; Makanya et al., 2009; Konerding et al., 2010; Paku et al., 2011; De Spiegelaere et al., 2012; Ribatti and Djonov 2012; Konerding et al., 2012; Ackermann et al., 2013; Mentzer and Konerding, 2014; Föhst et al., 2015; Díaz-Flores et al., 2016, 2017a,b, 2018a; Hlushchuk et al., 2017). In this order, in angiolipoma, these structures showed a) a cover formed by ECs and a core formed by pericytes and extracellular matrix in immunohistochemical and ultrastructural procedures, and b) a subsequent appearance and disappearance in serial visions, and three-dimensional reconstruction in confocal microscopy. Next, we consider the findings related to the tissue folds and, subsequently, to the commonly named pillars (<2.5 μm).

The presence of fibrin-platelet microthrombi in some vessels is a well-known and easily found feature in angiolipoma and is absent in ordinary lipoma (Charifa et al., 2021). These microthrombi occur in the networks of capillary-sized vessels and in the occasional higher caliber vessels that form the increased vasculature in angiolipoma. In our study, we demonstrate the endothelialization of the thrombus surface from reoriented cells of the vessel wall. A similar extension of vein intimal ECs surrounding fragments of fibrin thrombi has been described in the main vein of ovarian pedicle after ovariectomy (Patan et al., 2001a,b) and in veins affected by intravascular papillary endothelial hyperplasia (Díaz-Flores et al., 2021a). Delimited by the ECs, angiolipoma thrombi appear as projections in the vessel lumen and change from intraluminal to extraluminal, contacting the periendothelial space in the region between both sides in which the vessel ECs begin their reorientation around the thrombus. Therefore, the thrombi behave as provisional cores of the future

intraluminal tissue folds. It is well known that the thrombus components, fibrin, and platelet-releasing factors, act on EC and pericyte behavior (O'Byrne et al., 2000; Laurens et al., 2006; Yakovlev and Medved, 2009; Díaz-Flores et al., 2009; Yau et al., 2015; Hamilos et al., 2018). The possible role of these thrombus components on the formation of intraluminal tissue folds and pillars in angiolipoma requires further studies. Using immunohistochemical markers, we have observed expression for VEGF-A and TNFα in the intravascular tissue folds. Future studies of the gene expression of inflammatory, angiogenic and related thrombotic factors are also required.

In the successive phases or stages proposed for fold/pillar formation in IA is the incorporation of pericytes, fibroblasts, and collagen into the central virtual core formed between the ECs that contact opposite vessel walls (Burri and Tarek, 1990; Burri, 1990, 1992; Djonov et al., 2000a,b; Patan et al., 2001 a,b; Burri and Djonov, 2002; Djonov et al., 2002, 2003; Burri et al., 2004; Díaz-Flores et al., 2020d). In angiolipoma folds, invasion of pericytes from the periendothelial space into the thrombus and formation of extracellular matrix give rise to the mature core of the intravascular tissue fold, while the persistent limiting thrombus ECs form its cover. CD34+ stromal cells/telocytes (Faussone Pellegrini and Popescu, 2011; Manetti, 2021; Rosa et al., 2021a,b), an important perivascular cell in the adipose tissue (Díaz-Flores et al., 2020b), were rarely observed in the fold core. Therefore, there is scarce participation of these cells in IA mechanisms, unlike in sprouting angiogenesis (Díaz-Flores et al., 2020b).

The observation of peg-and-socket junctions between pericytes and ECs is striking and particularly common in the intraluminal tissue folds. This type of junction has been described between these cells (Allsopp and Gamble, 1979; Díaz-Flores et al., 2009; Bigler et al., 2016) and even between vascular smooth muscle cells and ECs (Díaz-Flores et al., 2011, 2012) in several conditions. Interestingly, the arrangement of pericytes (with contractile capacity) between both sides in which the ECs are reoriented to cover the thrombus, as well as the presence of numerous pericyte/EC peg-and-socket junctions in this region, suggest an action to control the space between both sides, where the thrombus contacts the vessel periendothelial layer. In the present work, some structures are suggestive of peg-and-socket junctions established between modified thrombotic platelets and the ECs that delimit the thrombus (platelets form the peg and ECs form the socket). This type of platelet/EC junction has already been described in other conditions of vessels with IA (Díaz-Flores et al., 2020c, 2021b).

The existence of frequent segmented tissue folds in vessels of angiolipomas is also an important fact. Indeed, this segmentation (fold formation from folds) contributes to increasing the fold path until the folds come into contact with other folds or with the opposite vessel wall, facilitating vessel division by these transluminal tissue folds (growth of the tissue folds by segmentation) (Patan, 2008). The insertion of thin pillars (<2.5 μm in diameter) between folds and between folds and the vessel wall also facilitates this process (Burri and Tarek, 1990; Burri, 1990; 1992; Djonov et al., 2000a,b, 2003; Patan et al., 2001a,b; Burri and Djonov, 2002; Burri et al., 2004).

In angiolipoma, pillars (<2.5 μm in diameter) show findings related to the widely described successive stages of formation (Burri and Tarek, 1990; Burri, 1992; Djonov et al., 2000a; Patan 2001a,b; Burri and Djonov 2002; Djonov et al., 2003; Burri et al., 2004). Thus, pillars appear as 1) endothelial extensions or protrusions, 2) EC bilayer (bilayer formation by endothelial intercellular junction reorganization and formation of a central virtual core) and pillar perforation (nascent or early pillars), 3) EC bilayer around collagen and pericytes or pericyte processes, which invade the pillar core (as mentioned above, in angiolipoma it is exceptional to observe other stromal cells in the pillar core); the collagen (predominantly collagen IV in angiolipoma) may be formed by a) transport into the centrally perforated endothelial bilayer, as has been observed in other conditions (Paku et al., 2011), b) formation from ECs of the pillar cover and pericytes of the pillar core, and c) by both mechanisms, and 4) EC bilayers surrounding a core increased in size (mainly by greater extracellular matrix formation). In this final stage, it is difficult to distinguish pillars from mature thin folds.

A previously undescribed fact in IA is the presence of stripes of electron-dense material in the lumen of vessels surrounding folds and pillars and extending to the vessel wall. The fold and pillar location, orientation, periodicity, and junctions, as well as the facilitation of EC contacts leading to the division of vessel lumen, are influenced by several factors, including hemodynamic conditions (Djonov et al., 2002; Turhan et al., 2008; Filipovic et al., 2009; Miele et al., 2009; Tsuda et al., 2009; Lee et al., 2011; Ackermann et al., 2013; Föhst et al., 2015), above all blood flow (Turhan et al., 2008; Tsuda et al., 2009; Lee et al., 2011; Ackermann et al., 2013), and the pressure exerted by pericytes or other interstitial cells (Burri and Djonov, 2002). The plasmatic electron-dense material could also be an important factor in the guidance and arrangement of intraluminal folds and pillars. The precise characterization of this plasma component requires further study.

From the findings of our study, the steps in the formation of intraluminal tissue folds can be summarized as follows (Fig. 10): a) microthrombus formation in capillaries, b) thrombus delimitation by ECs from the vessel wall, except in a region of the thrombus contacting with the periendothelial layer and the interstitium, located between the sides of the curved and reoriented vessel ECs to cover the thrombus, c) thrombus modifications with regression of most components, invasion of pericytes throughout the region

contacting with the periendothelial layer, and formation of extracellular matrix, d) numerous peg-and-socket junctions between pericytes and ECs, e) mature intraluminal tissue fold development, with a cover formed by the primitive and persistent thrombus-delimiting ECs, and a core formed by the penetrating pericytes and the newly formed extracellular matrix, f) intraluminal tissue fold contact with the opposite vessel wall and vessel division, and g) fold segmentation, which facilitates vessel division. In pillar formation, the following steps can be deduced: a) intraluminal extensions of ECs forming nascent pillars, b) EC bilayer arrangement of the extended ECs, c) extracellular matrix formation and pericyte process penetration between the EC bilayer, and d) larger pillars that can merge with intraluminal tissue folds and other pillars, leading to the division of vessel lumens. In addition, the ultrastructural observation of an electron-dense plasmatic material surrounding the intraluminal tissue folds and pillars, connecting them to each other and to the vessel wall, suggests the involvement of this material in the guidance and arrangement of intraluminal folds and pillars.

In conclusion, IA contributes to the development of the microvasculature in angiolipoma. Microthrombi, frequently observed in this lesion, are involved in the IA process. IA participation occurs through the formation of folds/pillars, which increase the microvascular network by dividing the vessel lumen. Folds/pillars are made up by an endothelial cell cover and a core. Clot components cooperate in the IA process forming a) a provisional core (replaced by a mature core after pericyte invasion and extracellular matrix formation) and b) intraluminal plasmatic electron-dense material, which surrounds folds/pillars and connects with the vessel wall, contributing to the connections and probably to the arrangement of these structures. Thus, the demonstration of IA and the events that occur during IA/thrombus association in angiolipoma have interest in the histogenesis of this pathological entity, easily found in pathology laboratory files, which therefore can be an affordable substrate for future studies on the action of clot components in IA, also of clinical and therapeutic interest.

*Acknowledgements.* The authors would like to thank Kim Eddy for the English revision.

Funding from University of La Laguna and Canary Council of Economy, Knowledge and Employment (CEI program) is acknowledged

*Conflicts of Interest.* The authors declare no conflict of interest.

## References

Ackermann M., Tsuda A., Secomb T.W., Mentzer S.J. and Konerding M.A. (2013). Intussusceptive remodeling of vascular branch angles in chemically-induced murine colitis. Microvasc. Res. 87, 75-82.

Ackermann M., Verleden SE., Kuehnel M., Haverich A., Welte T., Laenger F., Vanstapel A., Werlein C., Stark H., Tzankov A., Li WW., Li VW., Mentzer SJ. and Jonigk D. (2020). Pulmonary vascular endothelialitis, thrombosis, and angiogenesis in Covid-19. N. Engl. J. Med. 383, 120-128.

Allsopp G. and Gamble H.J. (1979). An electron microscopic study of the pericytes of the developing capillaries in human fetal brain and muscle. J. Anat. 128, 155-168.

Augustin H.G. (2001). Tubes, branches, and pillars: the many ways of forming a new vasculature. Circ. Res. 89, 645-647.

Bigler M., Koutsantonis D., Odriozola A., Halm S., Tschanz S.A., Zakrzewicz A., Weichert A. and Baum O. (2016). Morphometry of skeletal muscle capillaries: The relationship between capillary ultrastructure and ageing in humans. Acta Physiol. 218, 98-111.

Burri P.H. (1990). Development and growth of the respiratory system. Arch. Int. Physiol. Biochim. 98, A109-A111.

Burri P.H. (1992). Intussusceptive microvascular growth, a new mechanism of capillary network formation. EXS 61, 32-39.

Burri P.H. and Djonov V. (2002). Intussusceptive angiogenesis–the alternative to capillary sprouting. Mol. Aspects Med. 23, S1-27.

Burri P.H. and Tarek M.R. (1990). A novel mechanism of capillary growth in the rat pulmonary microcirculation. Anat. Rec. 228, 35-45.

Burri P.H., Hlushchuk R. and Djonov V. (2004). Intussusceptive angiogenesis: its emergence, its characteristics, and its significance. Dev. Dyn. 231, 474-488.

Caduff J.H., Fischer L.C. and Burri P.H. (1986). Scanning electron microscope study of the developing microvasculature in the postnatal rat lung. Anat. Rec. 216, 154-164.

Charifa A., Azmat C.E. and Badri T. (2021). Lipoma Pathology. In: StatPearls [Internet]. Treasure Island (FL): StatPearls Publishing.

De Spiegelaere W., Casteleyn C., Van den Broeck W., Plendl J., Bahramsoltani M., Simoens P., Djonov V. and Cornillie P. (2012). Intussusceptive angiogenesis: a biologically relevant form of angiogenesis. J. Vasc. Res. 49, 390-404.

Díaz-Flores L., Gutiérrez R., Madrid J.F., Varela H., Valladares F., Acosta E., Martín-Vasallo P. and Díaz-Flores L. Jr. (2009). Pericytes. Morphofunction, interactions and pathology in a quiescent and activated mesenchymal cell niche. Histol. Histopathol. 24, 909-969.

Díaz-Flores L., Jr., Gutiérrez R., Madrid J.F., Sáez F.J., Valladares F., Villar J. and Díaz-Flores L. (2011). Peg-and-socket junctions between smooth muscle cells and endothelial cells in femoral veins are stimulated to angiogenesis by prostaglandin $E_2$ and glycerols. Histol. Histopathol. 26, 623-630.

Díaz-Flores L., Gutiérrez R., García M.P., Díaz-Flores L. Jr., Valladares F. and Madrid J.F. (2012). Ultrastructure of myopericytoma: A continuum of transitional phenotypes of myopericytes. Ultrastruct. Pathol. 36, 189-194.

Díaz-Flores L., Gutiérrez R., Madrid J.F., García-Suárez M.P., González-Álvarez M.P., Díaz-Flores Jr L. and Sáez F.J. (2016). Intravascular papillary endothelial hyperplasia (IPEH). Evidence supporting a piecemeal mode of angiogenesis from vein endothelium, with vein wall neovascularization and papillary formation. Histol. Histopathol. 31, 1271-1279.

Díaz-Flores L., Gutiérrez R., García-Suárez M.P., Sáez F.J., Gutiérrez E., Valladares F., Carrasco J.L., Díaz-Flores Jr. L. and Madrid J.F. (2017a). Morphofunctional basis of the different types of angiogenesis and formation of postnatal angiogenesis-related secondary structures. Histol. Histopathol. 32, 1239-1279.

Díaz-Flores L., Gutiérrez R., García M.D.P., Sáez F.J., Díaz-Flores Jr. L. and Madrid J.F. (2017b). Piecemeal mechanism combining sprouting and intussusceptive angiogenesis in intravenous papillary

formation induced by PGE2 and glycerol. Anat. Rec. (Hoboken). 300, 1781-1792.

Díaz-Flores L., Gutiérrez R., González-Gómez M., García P., Sáez F.J., Díaz-Flores Jr. L., Carrasco J.L. and Madrid J.F. (2018a). Segmentation of dilated hemorrhoidal veins in hemorrhoidal disease. Cells Tissues Organs 205, 120-128.

Díaz-Flores L., Gutiérrez R., García M.ª.P., González-Gómez M., Sáez F.J., Díaz-Flores Jr. L., Carrasco J.L. and Madrid J.F. (2018b). Sinusoidal hemangioma and intravascular papillary endothelial hyperplasia: interrelated processes that share a histogenetic piecemeal angiogenic mechanism. Acta Histochem. 120, 255-262.

Díaz-Flores L., Gutiérrez R., González-Gómez M., García M.A.P., Carrasco J.L., Díaz-Flores L. Jr., Madrid J.F. and Álvarez-Argüelles H. (2020a). Participation of intussusceptive angiogenesis in the morphogenesis of lobular capillary hemangioma. Sci. Rep. 10, 4987.

Díaz-Flores L., Gutiérrez R., García M.P., González-Gómez M., Carrasco J.L., Alvarez-Argüelles H. and Díaz-Flores L. Jr. (2020b). Telocytes/CD34+ Stromal Cells in pathologically affected white adipose tissue. Int. J. Mol. Sci. 21, 9694.

Díaz-Flores L., Gutiérrez R., García M.P., Gayoso S., Carrasco J.L., Díaz-Flores L. Jr., González-Gómez M. and Madrid J.F. (2020c). Intussusceptive angiogenesis and peg-socket junctions between endothelial cells and smooth muscle cells in early arterial intimal thickening. Int. J. Mol. Sci. 21, 8049.

Díaz-Flores L., Gutiérrez R., Gayoso S., García M.P., González-Gómez M., Díaz-Flores L. Jr., Sánchez R., Carrasco J.L. and Madrid J.F. (2020d). Intussusceptive angiogenesis and its counterpart intussusceptive lymphangiogenesis. Histol Histopathol. 35, 1083-1103.

Díaz-Flores L., Gutiérrez R., González-Gómez M., García MP., Carrasco JL., Díaz-Flores L Jr. and Madrid JF. (2021a). Myriad pillars formed by intussusceptive angiogenesis as the basis of intravascular papillary endothelial hyperplasia (IPEH). IPEH is intussusceptive angiogenesis made a lesion. Histol. Histopathol. 36, 217-228.

Díaz-Flores L., Gutiérrez R., García M.P., González-Gómez M., Díaz-Flores L. Jr., Gayoso S., Carrasco J.L. and Álvarez-Argüelles H. (2021b). Ultrastructural study of platelet behavior and interrelationship in sprouting and intussusceptive angiogenesis during arterial intimal thickening formation. Int. J. Mol. Sci. 22, 13001.

Djonov V., Schmid M., Tschanz S.A. and Burri P.H. (2000a). Intussusceptive angiogenesis: its role in embryonic vascular network formation. Circ. Res. 86, 286-292.

Djonov V.G., Galli A.B. and Burri P.H. (2000b). Intussusceptive arborization contributes to vascular tree formation in the chick chorio-allantoic membrane. Anat Embryol (Berl). 202, 347-357.

Djonov V.G., Kurz H., Burri P.H. (2002). Optimality in the developing vascular system: branching remodeling by means of intussusception as an efficient adaptation mechanism. Dev. Dyn. 224, 391-402.

Djonov V., Baum O. and Burri P.H. (2003). Vascular remodeling by intussusceptive angiogenesis. Cell Tissue Res. 314, 107-117.

Eelen G., Treps L., Li X. and Carmeliet P. (2020). Basic and therapeutic aspects of angiogenesis updated. Circ. Res. 127, 310-329.

Faussone Pellegrini M.S. and Popescu L.M. (2011). Telocytes. Biomol. Concepts 2, 481-489.

Filipovic N., Tsuda A., Lee G.S., Miele L.F., Lin M., Konerding M.A. and Mentzer S.J. (2009). Computational flow dynamics in a geometric model of intussusceptive angiogénesis. Microvasc. Res. 78, 286-293.

Föhst S., Wagner W., Ackermann M., Redenbach C., Schladitz K., Wirjadi O., Ysasi A.B., Mentzer S.J. and Konerding M.A. (2015). Three-dimensional image analytical detection of intussusceptive pillars in murine lung. J. Microsc. 260, 326-337.

Folkman J. (1971). Tumor angiogenesis: therapeutic implications. N. Engl. J. Med. 285, 1182-1186.

Hamilos M., Petousis S. and Parthenakis F. (2018). Interaction between platelets and endothelium: from pathophysiology to new therapeutic options. Cardiovasc. Diagn. Ther. 8, 568-580.

Hlushchuk R., Styp-Rekowska B., Dzambazi J., Wnuk M., Huynh-Do U., Makanya A. and Djonov V. (2017). Endoglin inhibition leads to intussusceptive angiogenesis via activation of factors related to COUP-TFII signaling pathway. PLoS One 12, e0182813.

Karthik S., Djukic T., Kim J.D., Zuber B., Makanya A., Odriozola A., Hlushchuk R., Filipovic N., Jin S.W. and Djonov V. (2018). Synergistic interaction of sprouting and intussusceptive angiogenesis during zebrafish caudal vein plexus development. Sci. Rep. 8, 9840.

Konerding M.A., Gibney B.C., Houdek J.P., Chamoto K., Ackermann M., Lee G.S., Lin M., Tsuda A. and Mentzer S.J. (2012). Spatial dependence of alveolar angiogenesis in post-pneumonectomy lung growth. Angiogenesis 15, 23-32.

Konerding M.A., Turhan A., Ravnic D.J., Lin M., Fuchs C., Secomb T.W., Tsuda A. and Mentzer S.J. (2010). Inflammation-induced intussusceptive angiogenesis in murine colitis. Anat. Rec. (Hoboken). 293, 849-857.

Kurz H., Burri P.H. and Djonov V.G. (2003). Angiogenesis and vascular remodeling by intussusception: from form to function. News Physiol. Sci. 18, 65-70.

Laurens N., Koolwijk P. and de Maat M.P. (2006). Fibrin structure and wound healing. J. Thromb. Haemost. 4, 932-939.

Lee G.S., Filipovic N., Lin M., Gibney B.C., Simpson D.C., Konerding M.A., Tsuda A. and Mentzer S.J. (2011). Intravascular pillars and pruning in the extraembryonic vessels of chick embryos. Dev. Dyn. 240, 1335-1343.

Lin J.J. and Lin F. (1974). Two entities in angiolipoma. A study of 459 cases of lipoma with review of literature on infiltrating angiolipoma. Cancer 34, 720-727.

Makanya A.N., Hlushchuk R. and Djonov V.G. (2009). Intussusceptive angiogenesis and its role in vascular morphogenesis, patterning, and remodeling. Angiogenesis 12, 113-123.

Manetti M. (2021). Molecular morphology and function of stromal cells. Int. J. Mol. Sci. 22, 13422.

Mentzer S.J. and Konerding M.A. (2014). Intussusceptive angiogenesis: expansion and remodeling of microvascular networks. Angiogenesis 17, 499-509.

Miele L.F., Turhan A., Lee G.S., Lin M., Ravnic D., Tsuda A., Konerding M.A. and Mentzer S.J. (2009). Blood flow patterns spatially associated with platelet aggregates in murine colitis. Anat. Rec. (Hoboken). 292, 1143-1153.

O'Byrne K.J., Koukourakis M.I., Giatromanolaki A., Cox G., Turley H., Steward W.P., Gatter K. and Harris A.L. (2000). Vascular endothelial growth factor, platelet-derived endothelial cell growth factor and angiogenesis in non-small-cell lung cancer. Br. J. Cancer 82, 1427-1432.

Paku S., Dezso K., Bugyik E., Tóvári J., Tímár J., Nagy P., Laszlo V., Klepetko W. and Döme B. (2011). A new mechanism for pillar formation during tumor-induced intussusceptive angiogenesis:

inverse sprouting. Am. J. Pathol. 179, 1573-1585.

Patan S. (2008). Lycat and cloche at the switch between blood vessel growth and differentiation? Circ. Res. 102, 1005-1007.

Patan S., Alvarez M.J., Schittny J.C. and Burri P.H. (1992). Intussusceptive microvascular growth: a common alternative to capillary sprouting. Arch. Histol. Cytol. 55 (Suppl), 65-75.

Patan S., Haenni B. and Burri P.H. (1993). Evidence for intussusceptive capillary growth in the chicken chorio-allantoic membrane (CAM). Anat. Embryol. (Berl). 187, 121-130.

Patan S., Haenni B. and Burri P.H. (1996a). Implementation of intussusceptive microvascular growth in the chicken chorioallantoic membrane (CAM): 1. pillar formation by folding of the capillary wall. Microvasc. Res. 51, 80-98.

Patan S., Munn L.L. and Jain R.K. (1996b). Intussusceptive microvascular growth in a human colon adenocarcinoma xenograft: a novel mechanism of tumor angiogenesis. Microvasc. Res. 51, 260-272.

Patan S., Munn L.L., Tanda S., Roberge S., Jain R.K. and Jones R.C. (2001a). Vascular morphogenesis and remodeling in a model of tissue repair: blood vessel formation and growth in the ovarian pedicle after ovariectomy. Circ. Res. 89, 723-731.

Patan S., Tanda S., Roberge S., Jones R.C., Jain R.K. and Munn L.L. (2001b). Vascular morphogenesis and remodeling in a human tumor xenograft: blood vessel formation and growth after ovariectomy and tumor implantation. Circ. Res. 89, 732-739.

Ribatti D. and Crivellato E. (2012). Sprouting angiogenesis, a reappraisal. Dev. Biol. 372, 157-165.

Ribatti D. and Djonov V. (2012). Intussusceptive microvascular growth in tumors. Cancer Lett. 2012. 316, 126-131.

Rosa I., Faussone-Pellegrini M.S., Romano E., Ibba-Manneschi L., Matucci-Cerinic M. and Manetti M. (2021a). Impairment in the telocyte/CD34+ stromal cell network in human rheumatoid arthritis synovium. J. Cell Mol. Med. 25, 2274-2278.

Rosa I., Marini M. and Manetti M. (2021b). Telocytes: An emerging component of stem cell niche microenvironment. J. Histochem. Cytochem. 69, 795-818.

Tsuda A., Turhan A., Konerding M., Ravnic D., Hanidziar D., Lin M. and Mentzer, S.J. (2009). Bimodal oscillation frequencies of blood flow in the inflammatory colon microcirculation. Anat. Rec. (Hoboken). 292, 65-72.

Turhan A., Konerding M.A., Tsuda A., Ravnic D.J., Hanidziar D., Lin M. and Mentzer S.J. (2008). Bridging mucosal vessels associated with rhythmically oscillating blood flow in murine colitis. Anat. Rec. (Hoboken). 291, 74-82.

Yakovlev S. and Medved L. (2009). Interaction of fibrin(ogen) with the endothelial cell receptor VE-cadherin: localization of the fibrin-binding site within the third extracellular VE-cadherin domain. Biochemistry 48, 5171-5179.

Yau J.W., Teoh H. and Verma S. (2015). Endothelial cell control of thrombosis. BMC Cardiovasc. Disord. 15, 130.

Accepted July 1, 2022